Biophysical Chemistry 185 (2014) 58–69

Contents lists available at ScienceDirect

Biophysical Chemistry

journal homepage: http://www.elsevier.com/locate/biophyschem

# ATPγS competes with ATP for binding at Domain 1 but not Domain 2 during ClpA catalyzed polypeptide translocation

Justin M. Miller, Aaron L. Lucius *

*Department of Chemistry, The University of Alabama at Birmingham, 1530 3rd Ave S, Birmingham, AL 35294-1240, United States*

## HIGHLIGHTS

- The competition between ATP and ATPγS for ClpA binding is examined here.
- We show that ATPγS interacts with ClpA differently when ClpP is present.
- The results suggest that ATPγS binds to D1 with an affinity of ~6 μM, but binds substantially weaker to D2.

## GRAPHICAL ABSTRACT

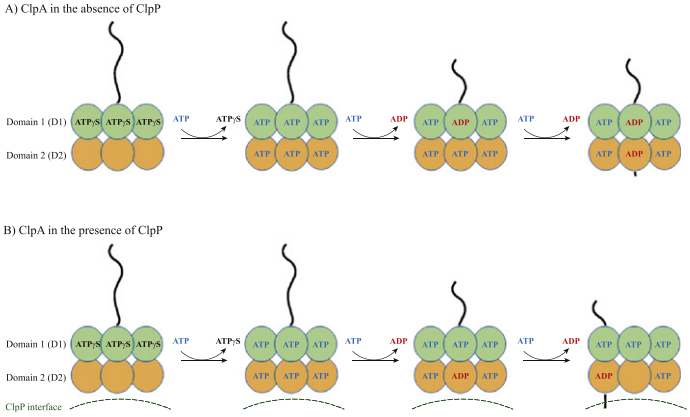


## ARTICLE INFO

*Article history:*
Received 18 September 2013
Received in revised form 1 November 2013
Accepted 1 November 2013
Available online 13 November 2013

*Keywords:*
ATP dependent proteases
AAA+ motor proteins
Pre-steady-state kinetics
Protein unfoldases
Steady-state kinetics

## ABSTRACT

ClpAP is an ATP-dependent protease that assembles through the association of hexameric rings of ClpA with the cylindrically-shaped protease ClpP. ClpA contains two nucleotide binding domains, termed Domain 1 (D1) or 2 (D2). We have proposed that D1 or D2 limits the rate of ClpA catalyzed polypeptide translocation when ClpP is either absent or present, respectively. Here we show that the rate of ClpA catalyzed polypeptide translocation depends on [ATPγS] in the absence of ClpP, but not in the presence of ClpP. We observe that ATPγS non-cooperatively binds to ClpA during polypeptide translocation with an apparent affinity of ~6 μM, but that introduction of ClpP shifts this affinity such that translocation is not affected. Interpreting these data with our proposed model for translocation catalyzed by ClpA vs. ClpAP suggests that ATPγS competes for binding at D1 but not at D2.


## 1. Introduction

AAA+ proteases are a ubiquitous class of ATP-driven enzymes that are required in all organisms for the removal of both misfolded and properly folded proteins as a means of cell cycle regulation [1,2]. One example is the *Escherichia coli* ATP-dependent protease ClpAP, which targets SsrA-polypeptides that have been tagged via the SsrA–SmpB system for degradation [3–5]. ClpAP shares structural homology with

*Abbreviations:* ATPγS, Adenosine 5′-[gamma-thio]-triphosphate; NLLS, nonlinear-least-squares; AMP-PNP, Adenosine 5′-(β,γ-imido)triphosphate; ATP, Adenosine 5′-triphosphate; ADP, Adenosine 5′-diphosphate; SSR, sum of squared residuals; D1, Domain 1; D2, Domain 2.

* Corresponding author. Tel.: +1 205 934 8096; fax: +1 205 934 2543.
*E-mail address:* allucius@uab.edu (A.L. Lucius).

0301-4622/$ – see front matter © 2013 Elsevier B.V. All rights reserved.
http://dx.doi.org/10.1016/j.bpc.2013.11.002

other ATP-dependent proteases where a hexameric ring of ClpA, a AAA+ protein (ATPases associated with various cellular activities), associates with one or both ends of the cylindrically-shaped protease ClpP, where ClpP contains serine protease active sites sequestered in its inner core away from bulk solvent [5–11]. Once associated with ClpP, ClpA is responsible for enzyme catalyzed protein unfolding and polypeptide translocation through repeated cycles of ATP binding and hydrolysis.

ClpA is a Class 1 HSP100/Clp protein unfoldase, where Class 1 indicates that each monomer contains two nucleotide binding domains [1]. In addition to other conserved domains, each nucleotide binding domain contains the canonical Walker A and Walker B motifs [2]. The two nucleotide binding domains are termed Domain 1 or 2, D1 or D2, respectively, and are each thought to serve a particular function. D1 is hypothesized to be primarily responsible for ClpA oligomerization, while D2 is thought to play a larger role in polypeptide translocation [12,13]. However, variants of ClpA that are deficient in ATP hydrolysis at either D1 or D2 both support polypeptide translocation, which likely indicates that both ATP hydrolysis sites are involved in translocation of polypeptide substrate. One model for polypeptide translocation proposes that loops formed between each Walker A and Walker B motif protrude into the axial channel of hexameric ClpA and make contact with polypeptide substrates. ATP hydrolysis then modulates up and down movement of the loops thereby translocating the polypeptide chain through the axial channel [14–16].

It has been well established that ClpA requires nucleotide binding to assemble into hexameric rings competent for association with ClpP [6,17]. As a consequence, 1–2 mM ATPγS is often used in experiments where there is a need to preassemble ClpA into hexameric rings [6,13,18–22]. In some cases, this preassembled complex is then mixed with hydrolysable ATP and it is assumed that the ATP will exchange with ATPγS, which is likely to be a good assumption. However, since the experiment is being carried out in the presence of both ATP and ATPγS, the observed reaction is occurring under conditions where ATP and ATPγS may compete for binding to ClpA. For example, in our previous examination of ClpA catalyzed polypeptide translocation, we prebound ClpA to a polypeptide substrate in the presence of 150 μM ATPγS [23]. The sample was then rapidly mixed with 10 mM ATP and protein trap, resulting in a final concentration of 75 μM ATPγS and 5 mM ATP (see Fig. 1 for schematic). In that study, even though the competition between ATP and ATPγS was not well understood, we chose to preincubate ClpA with an initial [ATPγS] of 150 μM to minimize the effect of competition between ATPγS and hydrolysable ATP upon rapid mixing of the two reactants, if such competition was present. Despite the large excess of ATP over ATPγS, competition between the two nucleotides for binding to ClpA may still occur.

With the objective of eliminating the competing nucleotide, we have also explored a number of other strategies to assemble ClpA to hexamers, prebind ClpA to polypeptide, and initiate polypeptide translocation. For example, we prebound ClpA to polypeptide in the presence

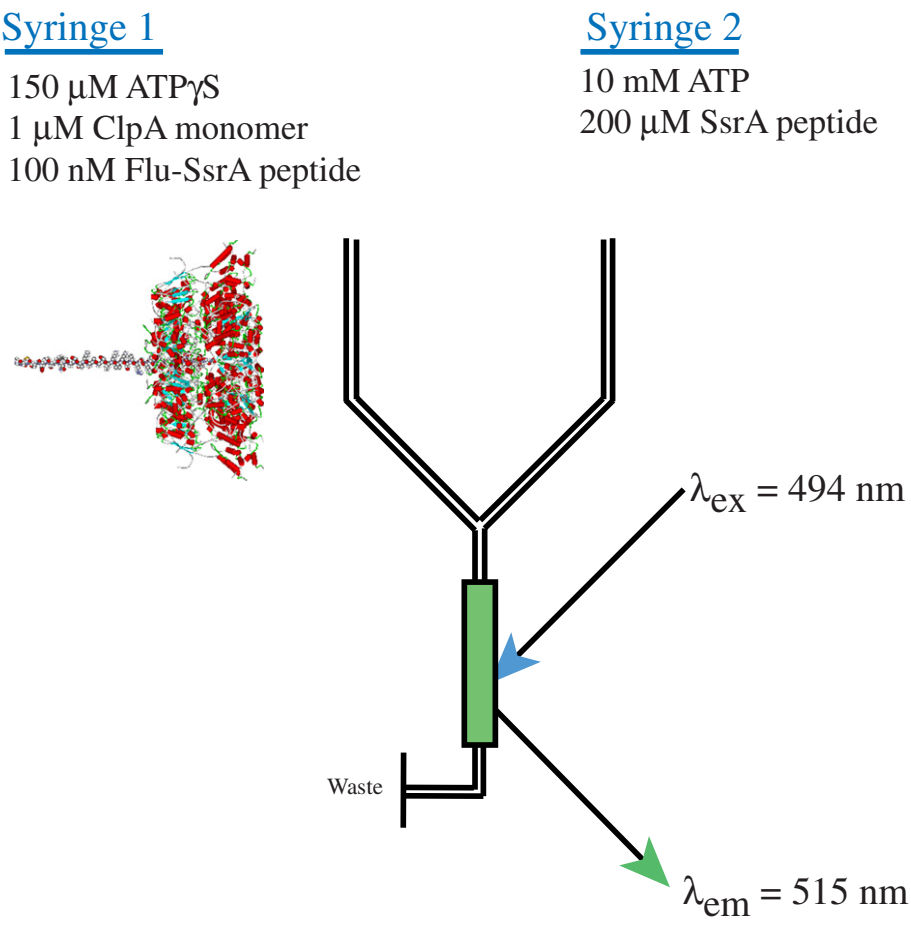


**Fig. 1.** Schematic representation of single turnover stopped-flow translocation experiments. Syringe 1 contains the indicated reagents, ClpA, ATPγS, and fluorescein-labeled polypeptide. The structure schematizes the contents of syringe 1 with ClpA hexamers bound by a single polypeptide. Syringe 2 contains 10 mM ATP and 200 μM SsrA peptide to serve as a trap for unbound ClpA or any ClpA that dissociates from polypeptide during the course of the reaction. The two reactants are rapidly mixed in the green colored chamber and fluorescein is excited at $\lambda_{ex} = 494$ nm. Fluorescein emission is observed above 515 nm with a 515 nm long pass filter. Upon mixing, the concentrations are two-fold lower than in the preincubation syringe.

of ATP and absence of $Mg^{2+}$ and attempted to initiate translocation by rapidly mixing with $Mg^{2+}$. However, no translocation was observed (unpublished result). Furthermore, we explored the possibility of assembling ClpA using a number of other nucleotides and nucleotide analogs. These included AMP-PNP, AMP-PCP, ADP, and ADP.BeF. In that study, we showed that only AMP-PNP would assemble a prebound complex that would initiate translocation [22]. However, substantially higher concentrations of AMP-PNP compared to ATPγS are required, which was consistent with previous reports on assembling ClpA with AMP-PNP [17]. Consequently, ATPγS has emerged as the most effective nucleotide analog for preassembling ClpA.

Despite ATPγS being the most effective nucleotide analog to assemble and prebind the complex, several concerns remain. First, ATPγS is slowly hydrolyzed by ClpA. This leads to the question; how fast is ATPγS hydrolyzed and, upon hydrolysis, does ATPγS provide sufficient energy to drive polypeptide translocation in the preincubation syringe? If this occurs, the population of enzyme may not all be bound at the SsrA tag at the carboxy terminus in the pre-incubation syringe (see syringe 1, Fig. 1). Rather, the enzyme may be distributed randomly on the polypeptide substrate upon rapid mixing with ATP. Second, does competition between ATPγS and ATP binding impact the reported kinetic parameters?

Here we report an examination of the effect of the ATP analog, ATPγS, on ClpA catalyzed polypeptide translocation in both the presence and absence of ClpP. We have employed our previously developed single turnover stopped-flow method to examine the kinetic parameters of ClpA catalyzed polypeptide translocation as a function of increasing ATPγS concentrations [23,24]. Our results show that in the presence of 1 mM ATPγS, the rate of polypeptide translocation is affected by competition between ATPγS and hydrolysable ATP binding to ClpA. However, this effect is not present upon addition of ClpP. These observations, when incorporated with our proposed mechanism for ClpA and ClpAP catalyzed polypeptide translocation [25], suggest that ATPγS competes for ATP binding at the D1 ATP binding site and therefore impacts polypeptide translocation catalyzed by ClpA in the absence of ClpP. No competition between ATP and ATPγS was observed when ClpP was present. Therefore, ATPγS does not appear to effectively compete for binding at the D2 ATP binding site.

## 2. Materials and methods

### 2.1. Materials

All solutions were prepared in double-distilled water produced from a Purelab Ultra Genetic system (Siemens Water Technology, Alpharetta, Georgia) using reagent grade chemicals purchased commercially. All peptide substrates were synthesized by CPC Scientific (Sunnyvale, CA), and were judged to be >90% pure by HPLC and mass spectral analysis. Fluorescein was covalently attached to the free cysteine residue at the amino terminus of the polypeptide as previously described. *E. coli* ClpA and ClpP were purified as previously described [25,39].

### 2.2. Methods

#### 2.2.1. ATPase activity assay

ATPγS hydrolysis was examined by pre-incubating 10 μM ClpA monomer in Buffer H (25 mM HEPES, pH 7.5 at 25 °C, 10 mM $MgCl_2$, 2 mM 2-mercaptoethanol, 300 mM NaCl, and 10% v/v glycerol) at 25 °C for 45 min prior to adding [$^{35}$S]-ATPγS. After 45 min, ATPγS that had been supplemented with [$^{35}$S]-ATPγS was added. For determination of the initial velocity, samples were removed and quenched with a 1:1 dilution of 1 M HCl. The pH of each sample was adjusted through addition of a solution containing 2.5 M NaOH, 0.5 M Tris, and 0.5 M EDTA such that the final pH was neutral. Reaction progress was monitored through separation of [$^{35}$S]-ATPγS from $^{35}$S-thio-phosphate using PEI-Cellulose F Thin Layer Chromatography plates (EMD Chemicals, Inc., Darmstadt, Germany) with 0.6 M $KH_2PO_4$ (pH 3.4 at 25 °C) as the mobile phase. TLC plates were exposed to a phosphor imager screen (Molecular Dynamics, Sunnyvale, CA) for a period of 90 min. Radioactive counts were then quantified using a Typhoon Trio+ (GE Healthcare, Piscataway, NJ) in phosphor storage mode using the 390 BP 100 phosphor filter. The resulting data was then processed using ImageQuant TL (GE Healthcare, Piscataway, NJ). The resulting initial velocities were plotted versus [ATPγS] and subjected to NLLS analysis using the Michaelis–Menten equation with no linear transformation, given by Eq. (1):

$$v_0 = \frac{k_{cat}[ClpA_{total}]}{1 + \frac{K_m}{[ATP\gamma S]}}. \quad (1)$$

#### 2.2.2. Stopped-flow fluorescence assay

Fluorescence stopped-flow experiments were performed as previously described and shown in Fig. 1. All reactions were prepared in buffer H (25 mM HEPES, pH 7.5 at 25 °C, 10 mM $MgCl_2$, 2 mM 2-mercaptoethanol, 300 mM NaCl, and 10% v/v glycerol). All experiments were performed in an SX.20 stopped-flow fluorometer (Applied Photophysics, Letherhead, UK). Prior to each reaction, 1 μM ClpA was preincubated with ATPγS for 25 min, concentration indicated in text. Fluorescently modified polypeptide substrate was then added such that the final concentration was 100 nM, and the mixture was loaded into syringe 1 of the stopped-flow fluorometer. Syringe 2 contained a solution of 10 mM ATP and 200 μM SsrA peptide prepared in buffer H. Prior to mixing, both solutions were incubated for an additional 10 min at 25 °C in the stopped-flow instrument. Increasing the incubation time of either solution in the stopped-flow instrument had no effect on the observed fluorescence time courses. Upon mixing, the final concentrations were 0.5 μM ClpA monomer, 50 nM peptide substrate, 100 μM SsrA peptide, 5 mM ATP, and the final concentration of ATPγS is indicated in the text. Fluorescein was excited at $\lambda_{ex} = 494$ nm and fluorescence emission was observed above 515 nm with a 515 nm long pass filter. All kinetic traces shown represent the average of at least 8 individual determinations.

Stopped-flow fluorescence experiments to examine ClpAP were performed in the presence of 1.2 μM ClpP. ClpAP was preassembled by incubating ClpA in the presence of ATPγS for 25 min, followed by incubation with ClpP for an additional 25 min. Fluorescently modified polypeptide substrate was then added such that the initial concentration was 20 nM, and the mixture was loaded into syringe 1 of the stopped-flow fluorometer.

#### 2.2.3. NLLS analysis

The system of coupled differential equations that result from Scheme 1 was solved using the method of Laplace transforms to obtain an expression for product formation as a function of the Laplace variable, $S(s)$, given by Eq. (2),

$$S(s) = \frac{1}{s}\left(\sum_{j=1}^{h}\frac{k_d k_C^{j-1}(k_{NP}+sx)}{(k_C+k_d+s)^j(k_{NP}+s)} + \sum_{i=1}^{n-1}\frac{k_d k_T^h k_T^{i-1}(k_{NP}+sx)}{(k_C+k_d+s)^h(k_{NP}+s)(k_d+k_T+s)^i} + \frac{(k_T+k_d)k_C^h k_T^{n-1}(k_{NP}+sx)}{(k_C+k_d+s)^h(k_{NP}+s)(k_d+k_T+s)^n}\right) \quad (2)$$

where capital $S$ represents the substrate and lower case $s$ is the Laplace variable, $h$ is the number of steps with rate constant $k_C$, $n$ is the number of steps with rate constant $k_T$, $k_{NP}$ is the rate of transition from a nonproductive complex to the productive complex, and $x$ is the fraction of ClpA bound in the productive form given by Eq. (3).

$$x = \frac{[ClpA \cdot S]_L}{[ClpA \cdot S]_L + [ClpA \cdot S]_{NP}}. \quad (3)$$

$$
\begin{array}{ccccccccc}
(E \bullet S)_{NP} & & & & & & & & \\
\downarrow k_{NP} & & & & & & & & \\
(E \bullet S)_L & \xrightarrow{k_c} & (E \bullet S)_L^1 & \xrightarrow{k_T} & I_{(L-m)} & \xrightarrow{k_T} & \ldots I_{(L-im)} \ldots & \xrightarrow{k_T} & E + S \\
\downarrow k_d & & \downarrow k_d & & \downarrow k_d & & \downarrow k_d & & \\
S & & S & & S & & S & &
\end{array}
$$

**Scheme 1.** Sequential *n*-step model for polypeptide translocation. $(E \cdot S)_L$ and $(E \cdot S)_{NP}$ represent enzyme bound to polypeptide substrate in the productive and nonproductive forms, respectively, and *S* is the unbound polypeptide substrate. $k_T$ is the translocation rate constant, $k_d$ is the dissociation rate constant, *L* is the polypeptide length, *m* is the average distance translocated between two rate limiting steps with rate constant $k_T$, '*i*' in $I_{(L\text{-}im)}$ represents *i* number of translocation steps, and the step that occurs with rate constant $k_c$ represents a step slower than the step with rate constant $k_T$.

Eq. (2) was then numerically solved using Eq. (4) to describe product formation as a function of time, $S(t)$,

$$S(t) = A_T \mathcal{L}^{-1} S(s) \tag{4}$$

where $A_T$ is the total amplitude of the time-course, and $\mathcal{L}^{-1}$ is the inverse Laplace transform operator. This was accomplished using the NLLS fitting routine, Conlin, and the inverse Laplace transform function using the IMSL C Numerical libraries (Visual Numerics, Houston, TX), as previously described [24,32]. Uncertainties reported on the parameters in Tables 2 and 3 and Fig. 4 are based on the average of a minimum of two experimental determinations.

The ATPγS concentration dependencies of the macroscopic rate of translocation and microscopic translocation rate constant displayed in Fig. 4a–b were subjected to NLLS analysis using an infinitely cooperative model given by Eq. (5),

$$mk_{T,app} = \frac{mk_{T,\max} \cdot (K_{ATP} \cdot [\mathrm{ATP}])^{\nu}}{1 + (K_{ATP} \cdot [\mathrm{ATP}])^{\nu} + \left(K_{ATP\gamma S} \cdot [\mathrm{ATP\gamma S}]\right)^{\omega}} \tag{5}$$

where $mk_{T,app}$ is the apparent macroscopic translocation rate. The maximum macroscopic translocation rate is represented as $mk_{T,max}$. The association equilibrium constants for ATP- or ATPγS-association with ClpA are represented as $K_{ATP}$ or $K_{ATP}\gamma_S$, respectively. The apparent Hill coefficients for nucleotide binding are represented by either $\nu$ or $\omega$ for ATP or ATPγS binding, respectively.

For translocation time courses collected in the presence of 75 μM ATPγS in the absence of ClpP, the "grid-searches" shown in Fig. 5b–c were performed by constraining either the kinetic step-size, *m*, or the elementary rate constant, $k_T$, to fixed values ranging from 1 to 40 or 0.35 to 10, in intervals of 0.04 or 0.01, respectively, followed by minimization of the SSR. For translocation time courses collected in the presence of 2.5 mM ATPγS in the absence of ClpP, the "grid-searches" shown in Fig. 5b–c were performed by constraining either the kinetic step-size, *m*, or the elementary rate constant, $k_T$, to fixed values ranging from 1 to 65 or 0.05 to 10, in intervals of 0.06 or 0.01, respectively, followed by minimization of the SSR. For translocation time courses collected in the presence of ClpA, ClpP, and 75 μM ATPγS, the "grid-searches" shown in Fig. 6b–c were performed by constraining either the kinetic step-size, *m*, or the elementary rate constant, $k_T$, to fixed values ranging from 2 to 21 or 0.6 to 10, in intervals of 0.04 or 0.01, respectively, followed by minimization of the SSR. For translocation time courses collected in the presence of ClpA, ClpP, and 1 mM ATPγS, the "grid-searches" shown in Fig. 6b–c were performed by constraining either the kinetic step-size, *m*, or the elementary rate constant, $k_T$, to fixed values ranging from 1.25 to 40 or 0.6 to 10, in intervals of 0.04 or 0.01, respectively, followed by minimization of the SSR.

## 3. Results

### 3.1. Kinetics of ATPγS hydrolysis catalyzed by ClpA

We first set out to determine the steady-state kinetic parameters, $K_m$ and $k_{cat}$, for ClpA catalyzed ATPγS hydrolysis. Experiments were performed by mixing 10 μM ClpA monomer with ATPγS supplemented with $^{35}$S-ATPγS (see Materials and methods). The total ATPγS concentration was varied between 100 μM and 1 mM. The initial velocity as a function of the total [ATPγS] is shown in Fig. 2a. The relationship between initial velocity and nucleotide concentration was subjected to NLLS analysis using Eq. (1) to obtain estimates of the Michaelis constant, $K_m = (134 \pm 46)$ μM, and the turnover number, $k_{cat} = (0.05 \pm 0.004)$ min$^{-1}$. Fig. 2a shows that ClpA hydrolyses ATPγS, albeit slowly.

The observation that ClpA hydrolyses ATPγS leads to the question; does hydrolysis of ATPγS provide sufficient energy to fuel polypeptide translocation? If ATPγS does provide sufficient energy for ClpA to translocate, then this would predict that not all of the ClpA in syringe 1 of Fig. 1 would be statically bound at the carboxy terminus of SsrA-tagged polypeptides. Rather, some molecules may have moved forward by some number of steps. If true, we would predict that the observed time courses would change depending on the amount of time the contents of syringe 1 (see Fig. 1) were allowed to incubate before rapid mixing with the contents of syringe 2. To test this, we collected time courses at various different incubation times. This was done because a time course is collected over a 400 s time period and up to ten time courses are collected. Thus, the contents of syringe 1 (Fig. 1) are allowed to incubate for up to 4000 s or 70 min by the time the last time course is collected. Fig. 2b shows two time courses collected using the experimental design schematized in Fig. 1, where 1 μM ClpA monomer has been allowed to incubate in the presence of 5 mM ATPγS and 100 nM fluorescein-labeled polypeptide for either ~15 (solid blue circles) or ~70 min (solid red circles) before mixing with ATP and SsrA peptide (pre-mixing concentrations).

If ATPγS hydrolysis provided enough energy to fuel polypeptide translocation, the extent of the lag would be expected to be decreased or nonexistent after ClpA had been incubated in the presence of 5 mM ATPγS and polypeptide for ~70 min. However, the time courses in Fig. 2b demonstrate that the extent of lag and the overall shape of the time courses are identical after 15 and 70 min of incubation in the presence of ATPγS. Thus, ClpA catalyzed hydrolysis of ATPγS does not impact the observed time courses for polypeptide translocation over this length of time. Consequently, the polypeptide substrates that are bound by ClpA in syringe 1 must represent hexameric ClpA bound at the SsrA sequence and not ClpA that has moved forward some distance.

### 3.2. Competition between ATP and ATPγS

Preassembling ClpA into hexameric rings using ATPγS is required to perform the single-turnover polypeptide translocation experiments reported here and previously [6,9,13,16,18,19,21–23]. Upon rapid

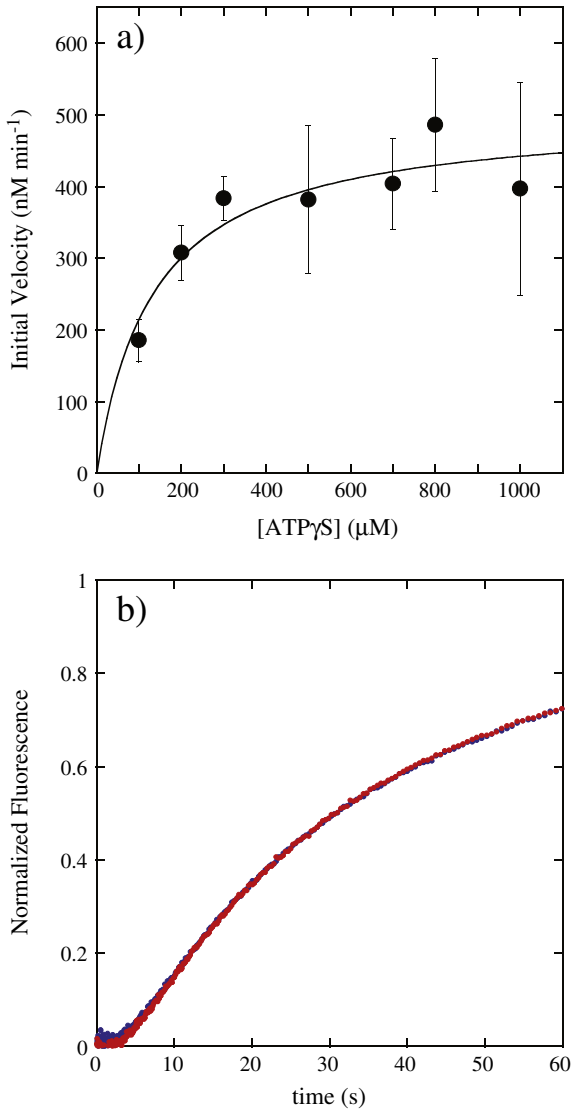


**Fig. 2.** ClpA catalyzes ATPγS hydrolysis. a) Steady-state kinetic experiments were performed by mixing 10 μM ClpA monomer with ATPγS supplemented with $^{35}$S-ATPγS. The relationship between initial velocity and nucleotide concentration was subjected to NLLS analysis using Eq. (1) to obtain estimates of the Michaelis constant, $K_m = (134 \pm 46)$ μM, and the turnover number, $k_{cat} = (0.05 \pm 0.004)$ min$^{-1}$. b) Two fluorescence time courses are shown that have been collected using the experimental design schematized in Fig. 1. ClpA has been allowed to incubate in the presence of 5 mM ATPγS and 100 nM fluorescein-labeled polypeptide for either ~15 (solid blue circles) or ~70 min (solid red circles) before mixing with ATP and SsrA peptide (pre-mixing concentrations).

mixing with hydrolysable ATP, it is likely that ATPγS and ATP compete for binding to ClpA. Moreover, this competition may impact the observed kinetic parameters. To elucidate the impact of the competition between ATP and ATPγS on the kinetic parameters, polypeptide translocation experiments were performed as a function of [ATPγS] by varying the concentration of ATPγS in the preincubation syringe (see Fig. 1, syringe 1).

Single turnover polypeptide translocation experiments were performed as described previously and in Materials and methods [23–25]. Syringe 1 of the stopped-flow is loaded with a solution containing 1 μM ClpA monomer, 100 nM fluorescein modified polypeptide substrate, and varying concentrations of ATPγS (see Fig. 1). Under the conditions illustrated in Fig. 1, the final mixing concentrations of ATPγS and ATP are 75 μM and 5 mM, respectively. Thus, the resultant time courses represent polypeptide translocation under conditions where ATPγS and ATP could compete for binding to ClpA.

Syringe 2 is loaded with a solution containing 10 mM ATP and 200 μM SsrA. The inclusion of a non-fluorescently modified SsrA polypeptide in syringe 2 serves as a protein trap that insures single-turnover conditions. Upon mixing of the contents of the two syringes, free ClpA or any ClpA that dissociates will rapidly bind the non-fluorescent SsrA trap, thus insuring that the observed signal is only sensitive to ClpA that was bound prior to mixing. Reaction progress is

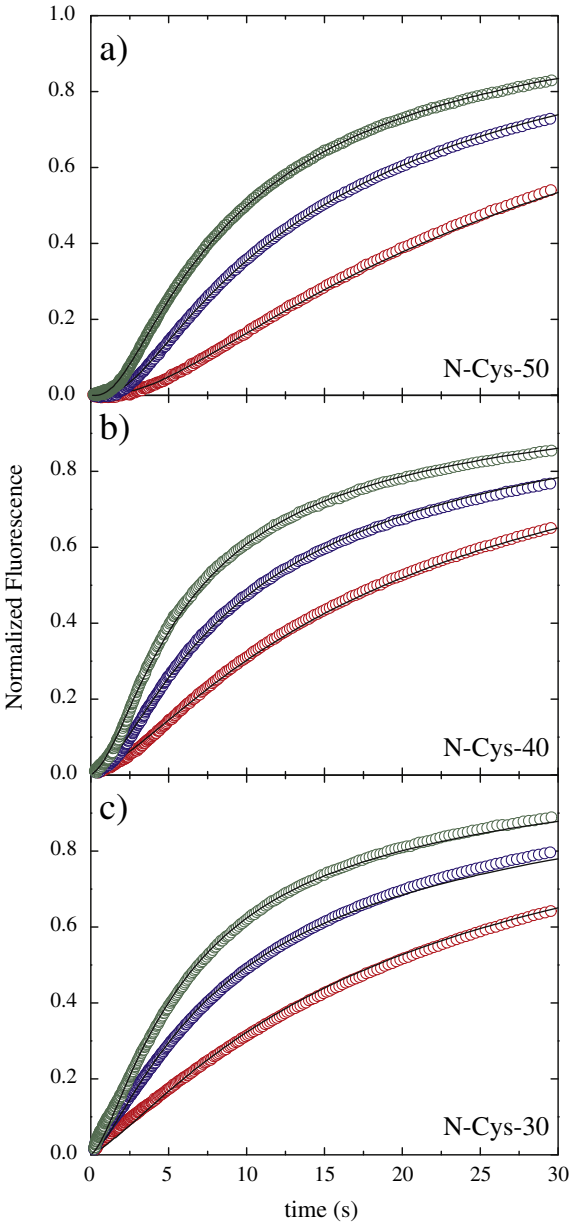


**Fig. 3.** Fluorescence time-courses for ClpA catalyzed polypeptide translocation. As shown in Fig. 1, 1 μM ClpA was pre-assembled in the presence of ATPγS and 100 nM fluorescein-labeled polypeptide substrate prior to rapidly mixing with 10 mM ATP and 200 μM SsrA. Time courses are shown for ClpA catalyzed polypeptide translocation of N-Cys-50, N-Cys-40, and N-Cys-30 (see Table 1) substrates after incubation of ClpA with 75 μM (green circles), 600 μM (blue circles), and 2.5 mM (red circles) ATPγS. The time courses shown illustrate that the extent of the lag phase is dependent upon [ATPγS]. The solid black lines represent a global NLLS fit using Scheme 1 for time-courses collected with substrates I–III in Table 1. The resulting kinetic parameters are summarized in Table 2 for each [ATPγS]. Each time-course was analyzed under a given set of conditions by constraining the parameters $k_T$, $k_C$, $k_{NP}$, and $h$ to be global parameters, while $A_x$, $x$, and $n$ were allowed to float for each polypeptide length.

monitored by exciting fluorescein at 494 nm and observing the emission at 515 nm and above using a 515 nm long pass filter.

Fig. 3 shows a representative set of time courses for translocation of ClpA on a set of polypeptide substrates that differ only in length in the presence of final mixing concentrations of 75 μM (green circles), 600 μM (blue circles) and 2.5 mM (red circles) ATPγS in the presence of a final concentration of 5 mM ATP. From qualitative inspection of the time courses shown in Fig. 3, it is clear that the rate of translocation is slowed with each increase in [ATPγS]. However, it is unclear if the apparent decrease in translocation rate is an effect of a change in the microscopic rate constants, kinetic step-size, or both.

### 3.3. Global NLLS analysis of translocation data

To quantify the effect of competition between ATP and ATPγS for binding to ClpA, single-turnover stopped-flow fluorescence experiments were performed as illustrated in Fig. 1. Experiments were carried out with substrates I–III (see Table 1) at final ATPγS concentrations of 75, 126, 250, 355, and 600 μM, and 1, 1.8, and 2.5 mM. Each set of time courses for three polypeptide lengths at a fixed ATPγS concentration was subjected to NLLS analysis to determine the parameters $k_T$, $m$, $mk_T$, $k_C$, and $k_{NP}$. The data were well described by Scheme 1 at all [ATPγS], and the resultant parameters are given in Table 2.

The macroscopic rate, $mk_T$, and the elementary rate constant, $k_T$, decrease with increasing [ATPγS] (see Fig. 4a–b). We previously reported a cooperative dependence of $mk_T$ and $k_T$ on [ATP] for ClpA catalyzed polypeptide translocation [23]. Consistently, those data were well described by an infinitely cooperative binding model with a Hill coefficient of ~2.5. In contrast, the dependencies of the kinetic parameters on [ATPγS] do not appear to exhibit isotherms consistent with cooperative binding of ATPγS (see Fig. 4 a–b). That is to say, from a qualitative inspection of the curves, the decreases in rate and rate constant with increasing [ATPγS] do not appear particularly steep.

To determine if cooperativity is present, the dependences of $mk_T$ and $k_T$ on [ATPγS] were subjected to NLLS analysis using an infinitely cooperative competition binding model given by Eq. (5) (see Materials and methods section). In Eq. (5), the parameters that define ATP binding were constrained to the previously determined values, specifically, $K_{ATP} = 1.9 \times 10^3\ M^{-1}$ ($K_{d,ATP} = 526$ μM) or $1.8 \times 10^3\ M^{-1}$ ($K_{d,ATP} = 556$ μM), the Hill coefficient for ATP binding, $\nu = 2.5$ or 2.2, for $mk_T$ or $k_T$, respectively and [ATP] = 5 mM. The floating parameters are the binding constant for ATPγS, $K_{ATP\gamma S}$, the Hill coefficient for ATPγS binding, $\omega$, and the maximum translocation rate or rate constant, $mk_{T,max}$ or $k_{T,max}$, respectively. For the analysis of $mk_T$ and $k_T$ (see Fig. 4a–b) the Hill coefficient for ATPγS was found to be $\omega = 0.88 \pm 0.03$ and $\omega = 1.2 \pm 0.2$, respectively. Since the values are close to one it was concluded that there is not significant cooperativity. Thus, the analysis was performed with the Hill coefficient for ATPγS binding constrained to one, i.e. $\omega = 1$ in Eq. (5). For the analysis of $mk_T$ (see Fig. 4a), estimates of the parameters were found to be $K_{ATP\gamma S} = (160 \pm 7) \times 10^3\ M^{-1}$ ($K_{d,ATP\gamma S} = (6.2 \pm 0.3)$ μM), and $mk_{T,max} = (21.6 \pm 0.2)$ aa $s^{-1}$.

The microscopic translocation rate constant, $k_T$, is plotted as a function of [ATPγS] in Fig. 4b. Similar to $mk_T$, the relationship between $k_T$ and [ATPγS] was subjected to NLLS analysis using Eq. (5) with $\omega = 1.0$. From this analysis the parameters $K_{ATP\gamma S}$ and $k_{T,max}$ were found to be $(104 \pm 13) \times 10^3\ M^{-1}$ ($K_{d,ATP\gamma S} = (10 \pm 1)$ μM) and $(1.39 \pm 0.05)\ s^{-1}$, respectively. The analysis of both $mk_T$ and $k_T$ shows that ATPγS binds to ClpA with nearly 100-fold greater affinity than ATP, but does so non-cooperatively [23]. This either indicates that the cooperativity is reduced in the presence of ATPγS or that ATPγS only binds to one of the two nucleotide binding sites on the ClpA monomer.

The kinetic step-size is plotted as a function of [ATPγS] in Fig. 4c and shows no significant dependence upon ATPγS concentration between 75 μM and 1 mM. However, at the two highest ATPγS concentrations, the parameter is between 20 and 24 aa $step^{-1}$ with large uncertainty. The kinetic step-size averaged over all eight ATPγS concentrations is $m = (18 \pm 3)$ aa $step^{-1}$, which is within error of our previously reported value of $m = (14 \pm 1)$ aa $step^{-1}$ independent of [ATP] [23]. At the two highest [ATPγS], 1.8 and 2.5 mM, the kinetic step-size is observed to increase. If these two data points are removed from the determination of the average, then $m = (16.3 \pm 0.5)$ aa $step^{-1}$.

### 3.4. Impact of parameter correlation on the determination of the kinetic parameters

We and others have reported that the elementary rate constant, $k_T$, and the kinetic step-size, $m$, are negatively correlated [23,26–28]. Because of this, under certain conditions it can be difficult to simultaneously determine both parameters. However, the overall rate of translocation, $mk_T$, contains less parameter correlation and tends to be a parameter that can be determined with higher precision [28,29]. This is a consequence of the fact that the overall rate, $mk_T$, represents the product of the kinetic step-size, $m$, and the elementary rate constant, $k_T$. In this study, both $mk_T$ and $k_T$ follow the same trend and are both well described by the same model. Thus, we asked the question; is the deviation in the kinetic step-size observed at high [ATPγS] a consequence of parameter correlation (see Fig. 4c)?

To assess the parameter correlation between the rate constant and the kinetic step-size, we performed Monte Carlo simulations (see Materials and methods). Fig. 5a is a plot of the translocation rate constant versus the kinetic step-size from two representative Monte Carlo simulations from polypeptide translocation experiments collected in the presence of 75 μM (solid blue spheres) and 2.5 mM (solid red spheres) ATPγS and a fixed [ATP] = 5 mM. Consistent with our previous report, in both cases, $k_T$ and $m$ are negatively correlated based on the observation of a negative slope (see Fig. 5a), where the slope represents the correlation coefficient. However, the 75 μM data exhibits a slope of $-0.096 \pm 0.001$ and the 2.5 mM data exhibits a slope of $-0.0148 \pm 0.0005$. If the two parameters had the same degree of correlation, one would expect the absolute value of the correlation coefficient to be −1. However, at both low and high [ATPγS], the correlation coefficient is less than one, in this case, indicating that the kinetic

**Table 1**
Polypeptide translocation substrates.

| Substrate | Name | Length (aa) | Sequence |
|---|---|---|---|
| I | N-Cys-50 | 50 | Flu-CLILHNKQLGMTGEVSFQAANTK SAANLKVKELRSKKKL**AANDENYALAA** |
| II | N-Cys-40 | 40 | Flu-CTGEVSFQAANTKSAANLKVKELRSK KKL**AANDENYALAA** |
| III | N-Cys-30 | 30 | Flu-CTKSAANLKVKELRSKKKL**AANDE NYALAA** |

Flu, Fluorescein dye covalently attached at the cysteine residue. In bold is the eleven amino acid SsrA sequence.

**Table 2**
ClpA polypeptide translocation parameters as a function of [ATPγS].

| | $m$ (aa $step^{-1}$) | $k_T$ ($s^{-1}$) | $mk_T$ (aa $s^{-1}$) | $k_{NP}$ ($s^{-1}$) | $k_C$ ($s^{-1}$) |
|---|---|---|---|---|---|
| *[ATPγS] (μM)* | | | | | |
| 75 | 16 ± 1 | 1.3 ± 0.1 | 20.8 ± 0.4 | 0.039 ± 0.002 | 0.15 ± 0.01 |
| 126 | 17 ± 1 | 1.2 ± 0.1 | 20.4 ± 0.1 | 0.034 ± 0.001 | 0.141 ± 0.004 |
| 250 | 17 ± 2 | 1.1 ± 0.1 | 18.6 ± 0.2 | 0.031 ± 0.001 | 0.125 ± 0.003 |
| 355 | 17 ± 2 | 1.1 ± 0.2 | 17.6 ± 0.4 | 0.029 ± 0.001 | 0.118 ± 0.003 |
| 600 | 16 ± 2 | 1.0 ± 0.1 | 15.7 ± 0.6 | 0.028 ± 0.001 | 0.102 ± 0.004 |
| *[ATPγS] (mM)* | | | | | |
| 1.0 | 16 ± 1 | 0.8 ± 0.1 | 13.1 ± 0.3 | 0.03 ± 0.01 | 0.089 ± 0.003 |
| 1.8 | 20 ± 3 | 0.5 ± 0.1 | 10.7 ± 0.3 | 0.0163 ± 0.0004 | 0.052 ± 0.001 |
| 2.5 | 24 ± 6 | 0.4 ± 0.1 | 9.1 ± 0.3 | 0.015 ± 0.001 | 0.043 ± 0.004 |

$k_T$ is the translocation rate constant, $k_C$ is an additional kinetic step defined by Scheme 1, $m$ is the kinetic step size, $k_{NP}$ is a slow conformational change defined by Scheme 1, and $mk_T$ is the macroscopic rate of translocation.

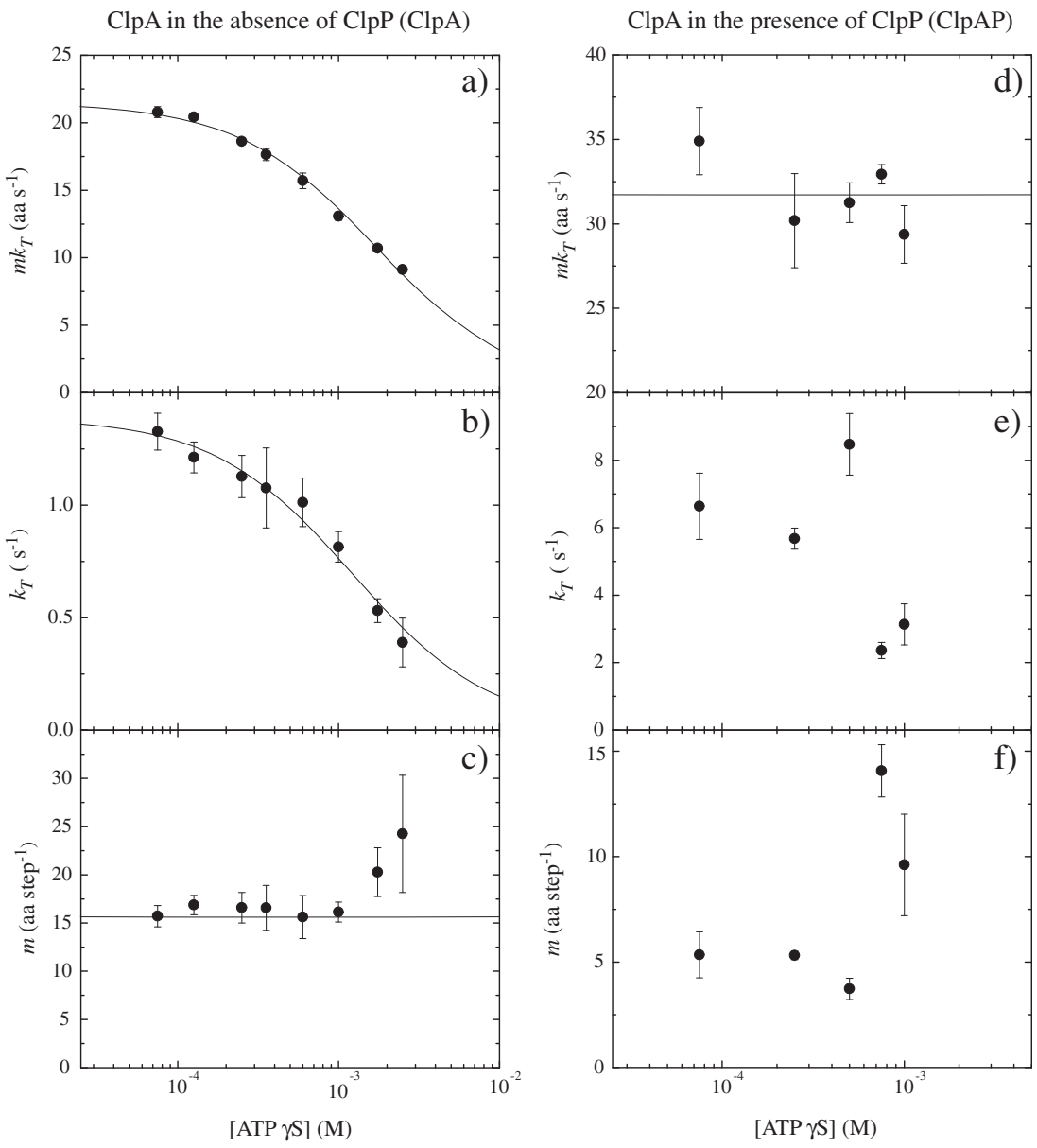


**Fig. 4.** Molecular mechanism for ClpA catalyzed polypeptide translocation depends on [ATPγS]. a) Dependence of $mk_T$ on [ATPγS] for ClpA catalyzed polypeptide translocation in the absence of ClpP, where the solid line is the result of a NLLS fit to Eq. (5) with $K_{ATP\gamma S} = (160 \pm 7) \times 10^3$ M$^{-1}$ and $mk_{T,max} = 21.6 \pm 0.2$ aa s$^{-1}$. The number of ATP and ATPγS binding sites, $\nu = 2.5$ and $\omega = 1.0$, respectively, the association equilibrium constant, $K_{ATP} = 1.9 \times 10^3$ M$^{-1}$, and [ATP] = 5 mM were treated as constant parameters in this analysis. b) The dependence of $k_T$ on [ATPγS] was subjected to NLLS analysis using Eq. (5), where the solid line represents the best fit with $K_{ATP\gamma S} = (104 \pm 13) \times 10^3$ M$^{-1}$ and $k_{T,max} = (1.39 \pm 0.05)$ s$^{-1}$. For this analysis, the number of ATP and ATPγS binding sites, $\nu = 2.2$ and $\omega = 1.0$, respectively, the association equilibrium constant, $K_{ATP} = 1.8 \times 10^3$ M$^{-1}$ and [ATP] = 5 mM were treated as constant parameters. c) Dependence of the kinetic step-size on [ATPγS], solid line represents the average of six measurements, $\langle m \rangle = (16.3 \pm 0.5)$ aa step$^{-1}$. (d) The rate of translocation for ClpA catalyzed polypeptide translocation in the presence of ClpP, $mk_T$, does not exhibit any dependence on ATPγS concentration with a mean $mk_T = (32 \pm 2)$ aa s$^{-1}$, where the solid line represents the average of five measurements. (e–f) The elementary rate constant and kinetic step-size for ClpA catalyzed polypeptide translocation in the presence of ClpP do not exhibit a significant dependence on [ATPγS].

step-size is less well constrained than the elementary rate constant. Furthermore, the observation of different correlation coefficients predicts a different degree of parameter correlation for data collected at low vs. high ATPγS concentrations. That is to say, for each incremental change in the elementary rate constant, a relatively large change in the kinetic steps-size will occur for the shallow slope exhibited at 2.5 mM ATPγS.

To assess how well the kinetic step-size is constrained, we examined the sum of the squared residuals (SSR) as a function of fixed values of the kinetic step-size for the two sets of data (see Fig. 5b). The minimum of these plots represent the best estimates of the kinetic step-size under conditions of 75 μM ATPγS (solid blue line) or 2.5 mM ATPγS (dashed red line). For plotting purposes, we have subtracted the value of the SSR at the minimum of each curve from each data point so the bottom of the parabola is close to zero (see Fig. 5b). Although both curves exhibit the expected concave up parabolic shape, the 2.5 mM ATPγS data exhibits a parabola with a broader minimum than the 75 μM ATPγS data. This observation is consistent with the slopes in the $k_T$ vs. $m$ plot shown in Fig. 5a. That is to say, a broad minimum in the parabola indicates that a wide range of kinetic step-sizes yield very similar SSR values.

In order to determine how well the elementary rate constant is constrained, we examined SSR as a function of fixed values of $k_T$ using the same methodology as applied to the assessment of the kinetic step-size. Similar to Fig. 5b, Fig. 5c shows a plot of SSR versus $k_T$ for both the 75 μM ATPγS (solid green line) and 2.5 mM ATPγS (solid red line) data sets. Both curves exhibit the expected concave up parabolic shape corresponding to the best estimate of the elementary rate

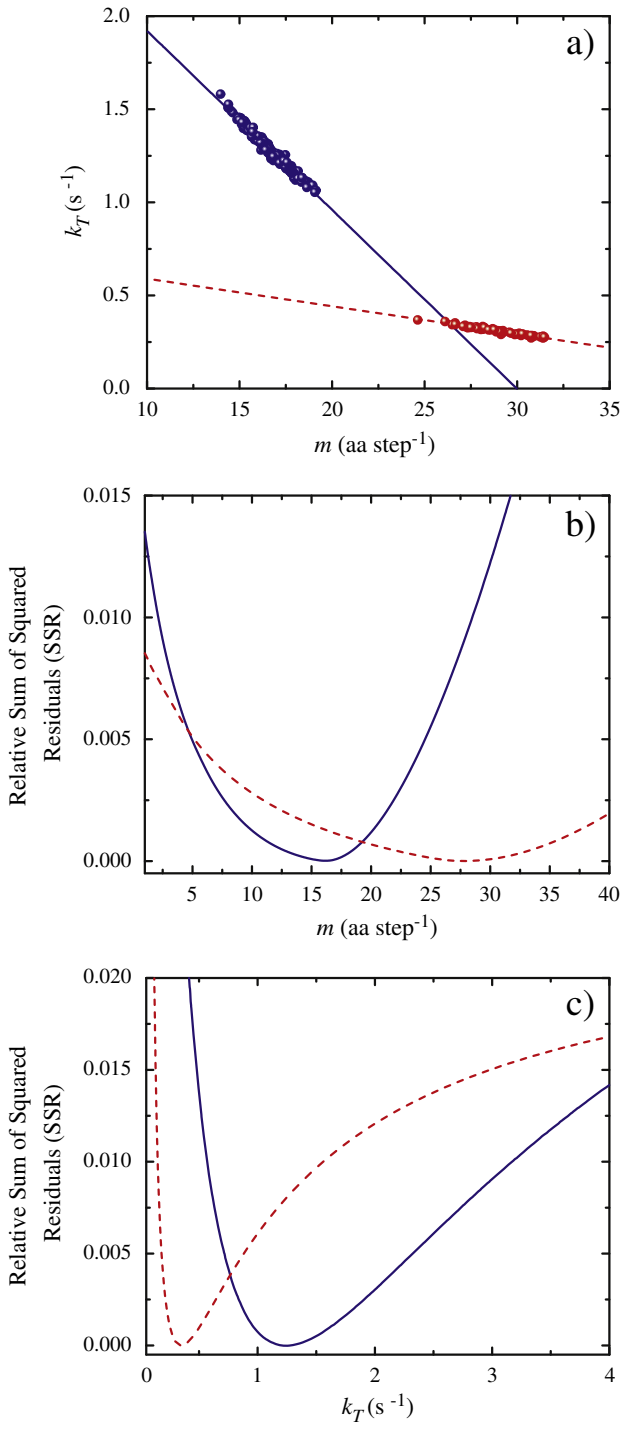


**Fig. 5.** Parameter correlation between the kinetic step-size and elementary rate constant depends on [ATPγS] for ClpA catalyzed polypeptide translocation in the absence of ClpP. (a) Plot of the translocation rate constant versus the kinetic step-size from two representative Monte Carlo simulations from polypeptide translocation experiments collected in the presence of 75 μM (blue spheres) and 2.5 mM (red spheres) ATPγS. Lines represent linear least-squares fit of 75 μM (solid blue line) and 2.5 mM (dashed red line) ATPγS data, where the 75 μM data exhibit a slope of $-0.096 \pm 0.001$ and the 2.5 mM data exhibit a slope of $-0.0148 \pm 0.0005$. (b, c) Plots of the sums of the squared residuals as functions of fixed values of the kinetic step-size (b) or fixed values for the elementary rate constant (c) for conditions of 75 μM (solid blue line) and 2.5 mM (dashed red line) ATPγS. From the minima shown in panel b, the best estimate of the kinetic step-size is $m = 16.2$ or 27.8 aa step$^{-1}$, for 75 μM or 2.5 mM ATPγS, respectively. For the elementary translocation rate constant, the best estimate from the minima shown in panel c is 1.2 s$^{-1}$ or 0.4 s$^{-1}$ for 75 μM or 2.5 mM ATPγS, respectively.

constant. From the minimum of each parabola, Fig. 5c shows that the minima in the SSR vs. $k_T$ plot is 1.2 s$^{-1}$ and 0.4 s$^{-1}$ for 75 μM and 2.5 mM ATPγS, respectively. However, the parabola corresponding to the 75 μM ATPγS dataset is observed to have a broader minimum than observed for the 2.5 mM ATPγS dataset, which is opposite to what was observed in the SSR vs. step-size plot in Fig. 5b. Thus, the elementary rate constant is better constrained at 2.5 mM ATPγS in comparison to 75 μM ATPγS, whereas the kinetic step-size is better constrained at 75 μM ATPγS and less well constrained at 2.5 mM ATPγS. These observations are consistent with the initial predictions made from the plot of $k_T$ versus $m$ shown in Fig. 5a.

These results indicate that at elevated [ATPγS], there is a change in the parameter correlation relative to low [ATPγS]. The consequence of this change is a reduced ability to uniquely determine the kinetic step-size at high [ATPγS]. Although the elementary rate constant is better constrained at high ATPγS concentrations, it is adequately constrained under both conditions.

### 3.5. ClpAP catalyzed polypeptide translocation

We recently reported that the kinetic step-size for ClpA when ClpP is present, i.e. ClpAP, is $(4.6 \pm 0.3)$ aa step$^{-1}$ compared to $(14 \pm 1)$ aa step$^{-1}$ for ClpA in the absence of ClpP [23]. Similarly, the translocation rate constant and the overall translocation rate were found to be $(7.9 \pm 0.2)$ s$^{-1}$ and $(36.1 \pm 0.7)$ aa s$^{-1}$, respectively, for ClpAP compared to ClpA alone where $k_T = (1.39 \pm 0.06)$ s$^{-1}$ and $mk_T = (19.5 \pm 0.7)$ aa s$^{-1}$ [23,25]. Moreover, the rate and rate constant for ClpA in the absence of ClpP exhibit a cooperative dependence on ATP concentration, whereas, ClpAP appears to depend non-cooperatively on ATP concentration. Since the molecular mechanisms for ClpA and ClpAP are emerging to be so different, we asked the question; does ClpAP exhibit the same dependence on [ATPγS] as ClpA in the absence of ClpP?

Single-turnover fluorescence stopped-flow experiments were performed as described in Fig. 1 with the modification that 1.2 μM ClpP was added to syringe 1 (see Fig. 1). Experiments were performed with substrates I–III at final ATPγS concentrations of 75, 250, 500, 750 and 1000 μM. All data were subjected to global NLLS analysis to determine the parameters $k_T$, $m$, $mk_T$, $k_C$, and $k_{NP}$ for each set of polypeptide lengths at each [ATPγS]. The data were well described by Scheme 1 at each [ATPγS]. The resultant parameters are summarized in Table 3 and plotted in Fig. 4d–f. Strikingly, the rate of translocation, $mk_T$, does not exhibit any dependence on ATPγS concentration. On the other hand, the three low ATPγS concentrations exhibit a rate constant, $k_T$, between 6 and 8 s$^{-1}$ within error of the value we have previously reported (see Fig. 4e). However, the rate constant drops to between 2 and 4 s$^{-1}$ at the two highest ATPγS concentrations. Similarly, the kinetic step-size also increases from a value of ~5 aa step$^{-1}$ to values of ~14 and 10 aa step$^{-1}$ at the two highest ATPγS concentrations. The observed change in the rate constant and kinetic step-size at 750 μM and 1 mM ATPγS is likely a consequence of parameter correlation since these two parameters are negatively correlated. Consistent with negative parameter correlation, the observed rate constant is observed to

**Table 3**
ClpAP polypeptide translocation parameters as a function of [ATPγS].

| [ATPγS] (μM) | $m$ (aa step$^{-1}$) | $k_T$ (s$^{-1}$) | $mk_T$ (aa s$^{-1}$) | $k_{NP}$ (s$^{-1}$) | $k_C$ (s$^{-1}$) |
|---|---|---|---|---|---|
| 75 | 5 ± 1 | 6.6 ± 0.9 | 35 ± 2 | 0.042 ± 0.002 | 0.23 ± 0.01 |
| 250 | 5.3 ± 0.2 | 5.7 ± 0.3 | 30 ± 3 | 0.033 ± 0.001 | 0.18 ± 0.01 |
| 500 | 4 ± 1 | 8.5 ± 0.9 | 31 ± 1 | 0.029 ± 0.001 | 0.17 ± 0.01 |
| 750 | 14 ± 1 | 2.4 ± 0.2 | 33 ± 1 | 0.0296 ± 0.0003 | 0.15 ± 0.002 |
| 1000 | 10 ± 2 | 3.1 ± 0.6 | 29 ± 2 | 0.026 ± 0.001 | 0.14 ± 0.002 |

$k_T$ is the translocation rate constant, $k_C$ is an additional kinetic step defined by Scheme 1, $m$ is the kinetic step size, $k_{NP}$ is a slow conformational change defined by Scheme 1, and $mk_T$ is the macroscopic rate of translocation.

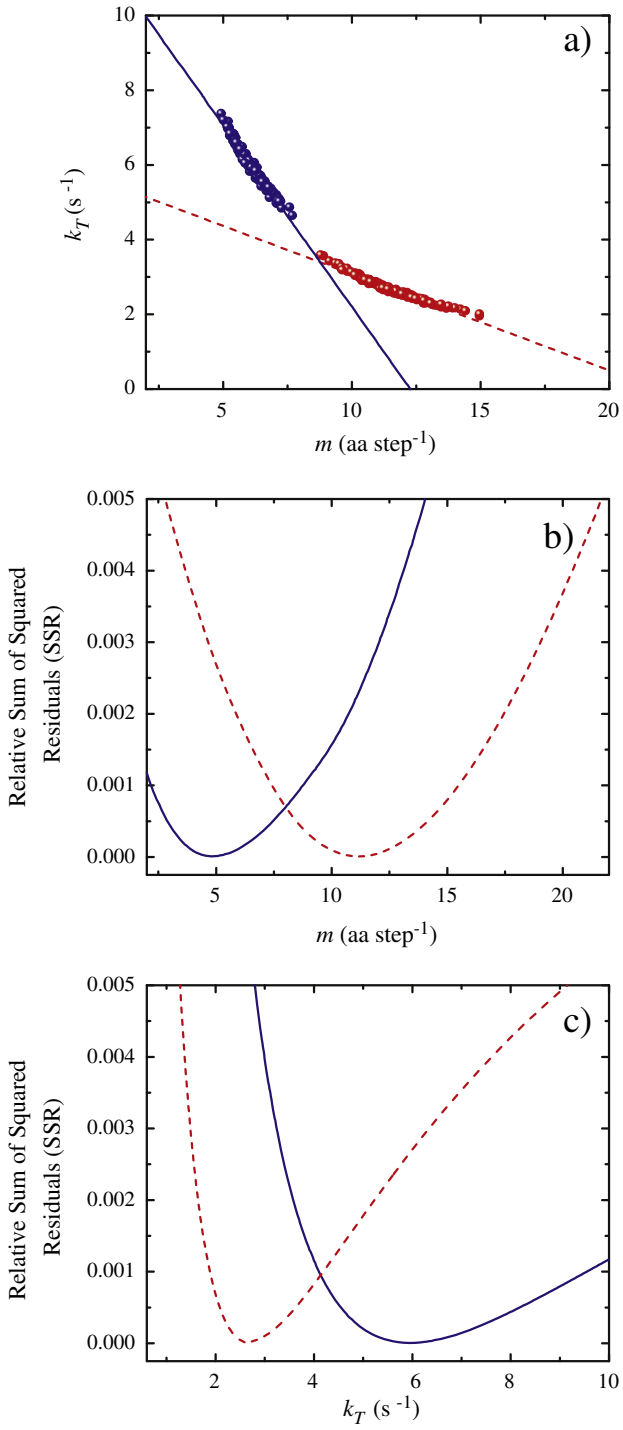


**Fig. 6.** Parameter correlation between the kinetic step-size and elementary rate constant depends on [ATPγS] for ClpA catalyzed polypeptide translocation in the presence of ClpP. (a) Plot of the translocation rate constant versus the kinetic step-size from two representative Monte Carlo simulations from polypeptide translocation experiments collected in the presence of 75 μM (blue spheres) and 1 mM (red spheres) ATPγS. Solid or dashed lines represent linear least-squares fit of 75 μM (solid blue line) and 1 mM (dashed red line) ATPγS data, where the 75 μM data exhibit a slope of $-0.97 \pm 0.01$ and the 1 mM data exhibit a slope of $-0.258 \pm 0.004$. (b, c) Plots of the sums of the squared residuals as functions of fixed values of the kinetic step-size (b) or fixed values for the elementary rate constant (c) for conditions of 75 μM (solid blue line) and 1 mM (dashed red line) ATPγS. From the minima shown in panel b, the best estimate of the kinetic step-size is $m = 4.8$ or 11.2 aa step$^{-1}$, for 75 μM or 1 mM ATPγS, respectively. For the elementary translocation rate constant, the best estimate from the minima shown in panel c is 5.9 s$^{-1}$ or 2.7 s$^{-1}$ for 75 μM or 1 mM ATPγS, respectively.

decrease and the kinetic step-size increase at the two highest concentrations of ATPγS. Also consistent with parameter correlation, the overall rate of translocation, $mk_T$ is not observed to depend on ATPγS over the range of [ATPγS] where both $k_T$ and $m$ do appear to change.

To determine whether the parameter correlation between the elementary rate constant and kinetic step-size is the same for both ClpA and ClpAP, we performed Monte Carlo simulations using ClpAP polypeptide translocation time courses. A plot of the resulting translocation rate constants versus the kinetic steps-size is shown in Fig. 6a, where representative Monte Carlo simulations are shown from polypeptide translocation experiments collected in the presence of 75 μM (solid blue spheres) and 1 mM (solid red spheres) ATPγS. As expected, the two parameters are negatively correlated for both 75 μM and 1 mM ATPγS. However, the correlation coefficients observed for ClpAP are different from the correlation coefficients observed for ClpA in the absence of ClpP (see Fig. 6a). For ClpAP, the 75 μM ATPγS data exhibit a slope of $-0.97 \pm 0.01$ and the 1 mM ATPγS data exhibit a slope of $-0.258 \pm 0.004$. Unlike ClpA in the absence of ClpP, ClpAP exhibits nearly 1:1 parameter correlation between $m$ and $k_T$ at 75 μM ATPγS. Although the correlation coefficient decreases to ~ −0.26 at 1 mM ATPγS, this correlation coefficient is approximately an order of magnitude larger than the correlation coefficient exhibited by ClpA in the absence of ClpP of ~ −0.015.

Fig. 6a predicts that the kinetic step-size should be better constrained at 75 μM ATPγS relative to 1 mM ATPγS. To test this hypothesis, we examined the SSR as a function of fixed values of the kinetic step-size for the two sets of data (see Fig. 6b). For plotting purposes, we have again subtracted the value of the SSR at the minimum of each curve from each data point so the bottom of the parabola is close to zero (see Fig. 6b). For both datasets, the plots of SSR versus $m$ exhibit the concave up parabolic shape that allows for the determination of the best estimate of the kinetic step-size. Although there is a decrease in the correlation coefficient of $k_T$ vs. $m$ in Fig. 6a, visually, there is not a substantial difference in the broadness of the minimum in the two SSR vs. $m$ plots shown in Fig. 6b. From the minima shown in Fig. 6b, the best estimate of the kinetic step-size is $m = 4.8$ or 11.2 aa step$^{-1}$ for 75 μM or 1 mM ATPγS, respectively.

To assess how well the elementary rate constant for ClpAP catalyzed polypeptide translocation is constrained under conditions of 75 μM ATPγS and 1 mM ATPγS, we examined SSR as a function of fixed values of $k_T$. Fig. 6c clearly shows that both curves exhibit the expected concave up shape. The parabola corresponding to the 75 μM ATPγS dataset (solid blue line) is observed to have a broader minimum than observed for the 1 mM ATPγS dataset (dashed red line). From this analysis the best estimate of the elementary rate constant is 5.9 s$^{-1}$ and 2.7 s$^{-1}$ for 75 μM and 1 mM ATPγS, respectively.

For both ClpA alone and for ClpA in the presence of ClpP, the degree of parameter correlation between $k_T$ and $m$ changes at the highest ATPγS concentrations. However, this transition is not observed to be as dramatic for ClpAP as it is for ClpA in the absence of ClpP. Although the kinetic parameters for ClpAP exhibit little ATPγS concentration dependence between 75 μM and 500 μM ATPγS some impact on the kinetic parameters is beginning to occur above 1 mM ATPγS (see Fig. 4d–f).

## 4. Discussion

Many studies, including ours, on proteolytic degradation by ClpAP and translocation by ClpA have reported results that come from experiments performed in the presence of ATPγS and ATP [8,19,21–23,30]. However, the potential competition between the nucleotide analog and ATP has not been addressed. The question is; does the inclusion of a particular ATP-analog affect the polypeptide binding or translocation activities of ClpA? We have previously reported that the nucleotide analogs ATPγS, AMP-PNP, AMP-PCP, ADP.BeF, and ADP promote the formation of ClpA hexamers, but only ATPγS and AMP-PNP promote

the formation of ClpA hexamers that are active in both polypeptide binding and translocation [22]. However, to fully populate hexamers, we [22], and others [17] have observed that higher concentrations of AMP-PNP are required relative to ATPγS. For this reason, ATPγS appears to be the only choice for efficiently pre-assembling and binding ClpA to a polypeptide substrate.

We previously reported an elementary rate constant, $k_T = (1.39 \pm 0.06)\ s^{-1}$, and overall rate, $mk_T = (19.4 \pm 1.3)$ aa $s^{-1}$, for ClpA catalyzed polypeptide translocation in the presence of 5 mM ATP and 75 μM ATPγS [23]. By examining the ATPγS concentration dependence of these parameters and extrapolating to zero ATPγS, here we have shown that the $k_T = (1.39 \pm 0.05)\ s^{-1}$ and $mk_T = (21.6 \pm 0.2)$ aa $s^{-1}$ in the presence of 5 mM ATP. Thus, these parameters are within error of our previous report [23]. Consequently, we conclude that the kinetic parameters previously reported reflect translocation under conditions where there is little to no competition between ATP and ATPγS. The same conclusion is drawn for ClpAP, since we have shown here that ClpA in the presence of ClpP exhibits no dependence on [ATPγS].

### 4.1. Model for polypeptide translocation catalyzed by ClpA vs. ClpAP

The strength of the single-turnover experiments applied here is that the kinetic time-courses are sensitive to the events in the active site of the enzyme and are not affected by macromolecular assembly or polypeptide binding. However, they are single-turnover with respect to polypeptide and multiple turnover with respect to ATP. That is to say, multiple rounds of ATP binding and hydrolysis are occurring during a single round of polypeptide translocation. Based on the observation of a lag in the single turnover kinetic time courses for polypeptide translocation, we can conclude that multiple steps with similar or the same rate constants are occurring before the enzyme dissociates.

For a motor protein to translocate a linear lattice, repetitive cycles of similar events must occur. At a minimum, this cycle must include ATP binding, hydrolysis, mechanical movement, ADP and $P_i$ release, and likely conformational changes. The single turnover experiments performed here are sensitive to the slowest repeating step in each of these cycles.

We have shown that, for both ClpA and ClpAP, the observed rate constant reflects a repeating step that immediately follows an ATP binding event within a cycle of translocation [23,25]. However, for ClpA this step repeats every ~14 amino acids translocated with an observed rate constant of ~1.39 $s^{-1}$ and for ClpAP this step repeats every ~2–5 amino acids translocated with an observed rate constant of ~6.6 $s^{-1}$. We have hypothesized that the rate limiting step that we observe for ClpA in the absence of ClpP is coupled to ATP hydrolysis site D1, and, when ClpP is present, the observed repeating rate-limiting step is coupled to D2. This hypothesis is based on our examination of the ATP concentration dependence of both the observed rate constant and the kinetic step-size [23,25], steady state ATP hydrolysis rates from Weber-Ban and coworkers [13], and crosslinking experiments from Horwich and coworkers [16].

To perform the single-turnover experiments reported here, we pre-bind ClpA to the polypeptide substrate. This is done to eliminate any effects on the kinetic time courses due to macromolecular assembly and polypeptide binding. To accomplish this, we must include a nucleotide analog to form hexameric rings competent for polypeptide binding [22]. In an attempt to eliminate the competing nucleotide analog, we have explored initiating translocation in a variety of other ways. For example, we have prebound ClpA to polypeptide in the presence of ATP and absence of $Mg^{2+}$ and attempted to initiate translocation by rapidly mixing with $Mg^{2+}$. However, no translocation was observed (unpublished result). In summary, we have found that ATPγS is the best and possibly the only practical option for pre-assembling and pre-binding ClpA to the polypeptide. Since we are "stuck" with ATPγS in these experiments, some of the experiments reported here were initiated to control for the fact that ATPγS may compete with ATP during repeating cycles of polypeptide translocation. Surprisingly, the results yielded insight into the differences in the molecular mechanism for ClpA vs. ClpAP catalyzed polypeptide translocation.

The examination of polypeptide translocation catalyzed by ClpA in the absence of ClpP as a function of [ATPγS] reveals that increasing concentrations of ATPγS slows down polypeptide translocation, which is an observation that has been reported [31]. Such an observation is not surprising and indicates that there is competition between ATP and ATPγS binding. More importantly, it indicates that there is competition between ATP and ATPγS at the ATP binding site that is responsible for coupling ATP binding and hydrolysis to polypeptide translocation.

As stated above, we have previously concluded that the repeating rate limiting step that limits the observation of translocation, in the absence of ClpP, is occurring at the D1 ATPase site. Thus, the competition between ATP and ATPγS is likely occurring at the D1 ATPase site. Further, the dependence of the rate and the observed rate constant on ATP exhibits a Hill coefficient of ~2.2 and 2.5, respectively. This indicates that there is cooperativity between ATP binding sites, which, by definition requires at least two ATP binding sites.

Unlike the previously reported dependence on [ATP], the translocation rate and rate constant do not exhibit cooperative dependencies on [ATPγS] for ClpA in the absence of ClpP. This observation suggests that ATPγS does not bind to both ATP binding sites on the monomer of ClpA or that binding to the second site is substantially weaker than the first. However, in order to observe a dependence on [ATPγS] the competition must occur at the site where the repeating rate limiting step is occurring and, based on our model, this site is most likely D1.

In contrast to ClpA alone, the translocation rate and rate constant for ClpA in the presence of ClpP exhibits little to no dependence on [ATPγS]. We have proposed that when ClpP is present, the observed repeating rate limiting step occurs at D2. Since we do not observe competition between ATP and ATPγS when ClpP is present, this is consistent with ATPγS binding more weakly to D2 than to D1.

It seems unlikely that ATPγS would not bind at all to D2, so we favor the interpretation that ATPγS binds more weakly to D2 than D1. Consistently, at 750 μM and 1 mM ATPγS, the kinetic step-size increases and the rate constant decreases, consistent with negative parameter correlation. Also consistent with parameter correlation is the fact that the overall rate does not appear to exhibit any dependence on [ATPγS] even at the most elevated concentrations.

### 4.2. Dependence of correlation coefficient on ATPγS

We, and others, have established that there is negative parameter correlation between the kinetic step-size and the elementary rate constant that is coupled to the observed kinetic step-size [3,24,26–28,32,33]. This can often lead to poor constraints on the two parameters and, under some conditions, the parameters cannot be simultaneously determined. Under such conditions, the overall rate, $mk_T$, is considered to be a more reliable parameter since the parameter correlation is largely canceled.

For ClpA in the absence of ClpP, the kinetic step-size increased to ~20 and ~24 at 1.8 and 2.5 mM ATPγS, respectively. With this observation in mind, we asked the question; is this simply due to parameter correlation or are we truly monitoring a different kinetic step that repeats every 20–25 amino acids. However, there is not a concomitant decrease in the observed rate constant or an effect on the overall rate. This is inconsistent with the typical effects of negative parameter correlation where it would be expected that the rate constant would decrease with a concomitant increase in the kinetic step-size. On the other hand, one may argue that the decrease in the rate constants is apparent in the data but the rate constant is already decreasing with increasing [ATPγS] and thus the effect is masked. If this were true, then the dependence of the rate constant on ATPγS would be steeper than the dependence of the overall rate on ATPγS. Upon inspection and comparison of

Fig. 4a–b, these two curves do not appear to exhibit vastly different midpoints.

We examined the parameter correlation between the kinetic step-size and the rate constant to determine if the observed change in the kinetic step-size is physically meaningful. Interestingly, the correlation coefficient changes quite significantly at the highest ATPγS concentrations. Specifically, the correlation coefficient is observed to decrease, which reduces the constraints on the kinetic step-size. Consequently, we do not interpret the increase in the kinetic step-size at 1.8 and 2.5 mM ATPγS to be physically meaningful. Rather, it is likely the consequence of the reduced constraints on the parameter.

Surprisingly, even though the kinetic parameters exhibit no dependence on [ATPγS] for ClpA in the presence of ClpP, the correlation coefficients does change with increasing [ATPγS] (see Supplemental Table S1). In the case of ClpAP, this indicates that, even though there is little effect on the kinetic parameters, there must still be some impact of high concentrations of ATPγS on translocation catalyzed by ClpAP. One possibility, among others, is that ATPγS binding to D1 may have some influence on translocation even though ATP hydrolysis at D2 is rate limiting. It is tempting to interpret the data in this way since the kinetic step-size increases to ~14 and ~10 aa step$^{-1}$ at 750 μM and 1 mM, respectively, and the rate constant decreases to 2.4 and 3.1 s$^{-1}$, respectively. The temptation occurs because these values are similar to the parameters observed for ClpA in the absence of ClpP, where we conclude that events occurring at D1 are rate limiting. However, due to the fact that the correlation coefficient decreases in this range, resulting in a reduction in the certainty on the kinetic step-size, one is required to conclude that these numbers may be fortuitously similar.

It is important to note that experiments performed at a final mixing concentration above 500 μM ATPγS are not likely to be conditions where we would examine the mechanism of polypeptide translocation. Although we preincubate ClpA with polypeptide substrate in the presence of 1 mM ATPγS, upon rapid mixing with ATP the final concentration of ATPγS is 500 μM. Such high concentrations of ATPγS were only used in this study to further probe the impact on the mechanism.

The single-turnover translocation experiments and the method of analysis presented here have been applied to polypeptide translocation [23–25], helicase catalyzed nucleic acid unwinding [34,35,27,33,36] and helicase catalyzed ssDNA translocation [28,37,38]. In all of these studies there is concern about the interpretation of the kinetic step-size and elementary rate constant since it is well known that the two parameters are negatively correlated. However, we contend that under many conditions these two parameters yield insight into the molecular mechanism. With the observation of the changes in the parameter correlation observed here, we propose that an examination of the parameter correlation should accompany the analysis of the kinetic parameters. This will allow the examiner to determine the range over which the parameters can be reliably interpreted.

### 4.3. Type 1 AAA + molecular chaperones

A major thrust of our research is to understand how Type 1 AAA + protein translocases coordinate the activity of their two ATP binding and hydrolysis sites per monomer (12 per hexamer) to polypeptide translocation. It is striking to us that the hexameric rings of Type 1 AAA + motors like ClpA, ClpB, Hsp104, NSF, and p97 all contain 12 ATP binding and hydrolysis sites per hexameric ring when most hexameric ring motor proteins only contain six. A fascinating question is; why the need for so many sites when many hexameric ring motors do their work with half as many? One potential answer is that the enzymatic activities of the different sets of nucleotide binding and hydrolysis sites are up-regulated or down-regulated depending upon which partner the enzyme is interacting with, i.e. ClpP and/or adapter proteins.

In a series of surprising observations, Wickner and coworkers showed that a mixture of ATP and ATPγS increased the activity of ClpB and Hsp104 catalyzed disaggregation and the rate of ATP hydrolysis [31]. That work represented the first report of a slowly hydrolysable nucleotide analog enhancing the activity of a motor protein. They went on to show, through mutational analysis of the D1 and D2 nucleotide binding sites, that ATPγS differentially competed for the two sites. Moreover, they concluded that ATPγS and cochaperone proteins could elicit similar impacts on ATP hydrolysis and disaggregation. These observations are similar to what we have observed here for ClpA. That is, our results support a hypothesis where D1 binds tighter to ATPγS than D2. Furthermore, if we think of ClpP as a cochaperone, the impact of ClpP on the activities of D1 and D2 are similar to how cochaperones impact ClpB activities.

Substantially more work is required on ClpA, ClpB, Hsp104, and other Type 1 AAA + motors, to fully understand the role of the D1 and D2 ATP binding and hydrolysis sites. It remains unclear how the two sites coordinate their activities and couple binding and hydrolysis to polypeptide translocation and/or disaggregation.

Supplementary data to this article can be found online at http://dx.doi.org/10.1016/j.bpc.2013.11.002.

## Acknowledgments

We would like to thank Clarissa Weaver and Ryan Stafford for comments on this manuscript. We would also like to thank to J. Woody Robins for use of the fermenter core facility. This work was supported by NSF grant MCB-0843746 to ALL, National Institute of Biomedical Imaging and Bioengineering (NIBIB) grant number T32EB004312 to JMM, and the University of Alabama at Birmingham Department of Chemistry. The content discussed here is solely the responsibility of the authors and does not necessarily represent the official views of the National Institute of Biomedical Imaging and Bioengineering or the National Institutes of Health.

## References

[1] B. Alberts, The cell as a collection of protein machines: preparing the next generation of molecular biologists, Cell 92 (1998) 291–294.
[2] A.F. Neuwald, L. Aravind, J.L. Spouge, E.V. Koonin, AAA+: a class of chaperone-like ATPases associated with the assembly, operation, and disassembly of protein complexes, Genome Res. 9 (1999) 27–43.
[3] A.W. Karzai, E.D. Roche, R.T. Sauer, The SsrA–SmpB system for protein tagging, directed degradation and ribosome rescue, Nat. Struct. Biol. 7 (2000) 449–455.
[4] S. Gottesman, Proteases and their targets in *Escherichia coli*, Annu. Rev. Genet. 30 (1996) 465–506.
[5] R.T. Sauer, T.A. Baker, AAA+ proteases: ATP-fueled machines of protein destruction, Annu. Rev. Biochem. 80 (2011) 587–612.
[6] J.R. Hoskins, M. Pak, M.R. Maurizi, S. Wickner, The role of the ClpA chaperone in proteolysis by ClpAP, Proc. Natl. Acad. Sci. U. S. A. 95 (1998) 12135–12140.
[7] S. Licht, I. Lee, Resolving individual steps in the operation of ATP-dependent proteolytic molecular machines: from conformational changes to substrate translocation and processivity, Biochemistry 47 (2008) 3595–3605.
[8] M.W. Thompson, S.K. Singh, M.R. Maurizi, Processive degradation of proteins by the ATP-dependent Clp protease from *Escherichia coli*. Requirement for the multiple array of active sites in ClpP but not ATP hydrolysis, J. Biol. Chem. 269 (1994) 18209–18215.
[9] Z. Maglica, K. Kolygo, E. Weber-Ban, Optimal efficiency of ClpAP and ClpXP chaperone-proteases is achieved by architectural symmetry, Structure 17 (2009) 508–516.
[10] M.R. Maurizi, S.K. Singh, M.W. Thompson, M. Kessel, A. Ginsburg, Molecular properties of ClpAP protease of *Escherichia coli*: ATP-dependent association of ClpA and clpP, Biochemistry 37 (1998) 7778–7786.
[11] T. Ishikawa, F. Beuron, M. Kessel, S. Wickner, M.R. Maurizi, A.C. Steven, Translocation pathway of protein substrates in ClpAP protease, Proc. Natl. Acad. Sci. U. S. A. 98 (2001) 4328–4333.
[12] S.K. Singh, M.R. Maurizi, Mutational analysis demonstrates different functional roles for the two ATP-binding sites in ClpAP protease from *Escherichia coli*, J. Biol. Chem. 269 (1994) 29537–29545.
[13] W. Kress, H. Mutschler, E. Weber-Ban, Both ATPase domains of ClpA are critical for processing of stable protein structures, J. Biol. Chem. 284 (2009) 31441–31452.
[14] F. Guo, M.R. Maurizi, L. Esser, D. Xia, Crystal structure of ClpA, an Hsp100 chaperone and regulator of ClpAP protease, J. Biol. Chem. 277 (2002) 46743–46752.

[15] J. Bohon, L.D. Jennings, C.M. Phillips, S. Licht, M.R. Chance, Synchrotron protein footprinting supports substrate translocation by ClpA via ATP-induced movements of the D2 loop, Structure 16 (2008) 1157–1165.
[16] J. Hinnerwisch, W.A. Fenton, K.J. Furtak, G.W. Farr, A.L. Horwich, Loops in the central channel of ClpA chaperone mediate protein binding, unfolding, and translocation, Cell 121 (2005) 1029–1041.
[17] M.R. Maurizi, ATP-promoted interaction between Clp A and Clp P in activation of Clp protease from *Escherichia coli*, Biochem. Soc. Trans. 19 (1991) 719–723.
[18] J.R. Hoskins, S.K. Singh, M.R. Maurizi, S. Wickner, Protein binding and unfolding by the chaperone ClpA and degradation by the protease ClpAP, Proc. Natl. Acad. Sci. U. S. A. 97 (2000) 8892–8897.
[19] K. Kolygo, N. Ranjan, W. Kress, F. Striebel, K. Hollenstein, K. Neelsen, M. Steiner, H. Summer, E. Weber-Ban, Studying chaperone-proteases using a real-time approach based on FRET, J. Struct. Biol. 168 (2009) 267–277.
[20] W. Kress, H. Mutschler, E. Weber-Ban, Assembly pathway of an AAA+ protein: tracking ClpA and ClpAP complex formation in real time, Biochemistry 46 (2007) 6183–6193.
[21] B.G. Reid, W.A. Fenton, A.L. Horwich, E.U. Weber-Ban, ClpA mediates directional translocation of substrate proteins into the ClpP protease, Proc. Natl. Acad. Sci. U. S. A. 98 (2001) 3768–3772.
[22] P.K. Veronese, B. Rajendar, A.L. Lucius, Activity of *Escherichia coli* ClpA bound by nucleoside di- and triphosphates, J. Mol. Biol. 409 (2011) 333–347.
[23] B. Rajendar, A.L. Lucius, Molecular mechanism of polypeptide translocation catalyzed by the *Escherichia coli* ClpA protein translocase, J. Mol. Biol. 399 (2010) 665–679.
[24] A.L. Lucius, J.M. Miller, B. Rajendar, Application of the sequential n-step kinetic mechanism to polypeptide translocases, Methods Enzymol. 488 (2011) 239–264.
[25] J.M. Miller, J. Lin, T. Li, A.L. Lucius, *E. coli* ClpA catalyzed polypeptide translocation is allosterically controlled by the protease ClpP, J. Mol. Biol. 425 (2013) 2795–2812.
[26] A.L. Lucius, C. Jason Wong, T.M. Lohman, Fluorescence stopped-flow studies of single turnover kinetics of *E. coli* RecBCD helicase-catalyzed DNA unwinding, J. Mol. Biol. 339 (2004) 731–750.
[27] A.L. Lucius, T.M. Lohman, Effects of temperature and ATP on the kinetic mechanism and kinetic step-size for *E. coli* RecBCD helicase-catalyzed DNA unwinding, J. Mol. Biol. 339 (2004) 751–771.
[28] C.J. Fischer, T.M. Lohman, ATP-dependent translocation of proteins along single-stranded DNA: models and methods of analysis of pre-steady state kinetics, J. Mol. Biol. 344 (2004) 1265–1286.
[29] C.J. Fischer, L. Wooten, E.J. Tomko, T.M. Lohman, Kinetics of motor protein translocation on single-stranded DNA, Methods Mol. Biol. 587 (2010) 45–56.
[30] M.W. Thompson, M.R. Maurizi, Activity and specificity of *Escherichia coli* ClpAP protease in cleaving model peptide substrates, J. Biol. Chem. 269 (1994) 18201–18208.
[31] S.M. Doyle, J. Shorter, M. Zolkiewski, J.R. Hoskins, S. Lindquist, S. Wickner, Asymmetric deceleration of ClpB or Hsp104 ATPase activity unleashes protein-remodeling activity, Nat. Struct. Mol. Biol. 14 (2007) 114–122.
[32] A.L. Lucius, N.K. Maluf, C.J. Fischer, T.M. Lohman, General methods for analysis of sequential "n-step" kinetic mechanisms: application to single turnover kinetics of helicase-catalyzed DNA unwinding, Biophys. J. 85 (2003) 2224–2239.
[33] A.L. Lucius, A. Vindigni, R. Gregorian, J.A. Ali, A.F. Taylor, G.R. Smith, T.M. Lohman, DNA unwinding step-size of *E. coli* RecBCD helicase determined from single turnover chemical quenched-flow kinetic studies, J. Mol. Biol. 324 (2002) 409–428.
[34] E. Jankowsky, C.H. Gross, S. Shuman, A.M. Pyle, The DExH protein NPH-II is a processive and directional motor for unwinding RNA, Nature 403 (2000) 447–451.
[35] J.A. Ali, T.M. Lohman, Kinetic measurement of the step size of DNA unwinding by *Escherichia coli* UvrD helicase, Science 275 (1997) 377–380.
[36] R. Galletto, M.J. Jezewska, W. Bujalowski, Unzipping mechanism of the double-stranded DNA unwinding by a hexameric helicase: quantitative analysis of the rate of the dsDNA unwinding, processivity and kinetic step-size of the *Escherichia coli* DnaB helicase using rapid quench-flow method, J. Mol. Biol. 343 (2004) 83–99.
[37] C.J. Fischer, N.K. Maluf, T.M. Lohman, Mechanism of ATP-dependent translocation of *E. coli* UvrD monomers along single-stranded DNA, J. Mol. Biol. 344 (2004) 1287–1309.
[38] L.T. Chisty, C.P. Toseland, N. Fili, G.I. Mashanov, M.S. Dillingham, J.E. Molloy, M.R. Webb, Monomeric PcrA helicase processively unwinds plasmid lengths of DNA in the presence of the initiator protein RepD, Nucleic Acids Res. 41 (2013) 5010–5023.
[39] P.K. Veronese, R.P. Stafford, A.L. Lucius, The *Escherichia coli* ClpA molecular chaperone self-assembles into tetramers, Biochemistry 48 (2009) 9221–9233.